

SUPERNOVA SHOCK TRIGGERING AND RADIOISOTOPE INJECTION INTO THE PRESOLAR CLOUD: EFFECTS OF ROTATIONAL AXIS ORIENTATION. Alan P. Boss & Sandra A. Keiser, DTM, Carnegie Institution (boss@dtm.ciw.edu).

Radio and sub-millimeter observations of the Type II supernova (SNe) remnant (SNR) W44 and its interaction with the W44 giant molecular cloud complex imply the presence of dense clumps of molecular gas that have been struck and compressed to sizes much less than 0.3 pc by the SNR shock front, with shock speeds of 20 to 30 km s⁻¹ [1,2]. HST images of the Cygnus Loop Type II SNR reveal shock front thicknesses of order 2×10^{-4} pc [3]. Detailed 2D [4] and 3D [5-7] hydrodynamical models of shock waves with these speeds and thicknesses have demonstrated the viability of triggered collapse of dense cloud cores with simultaneous injection of shock front material into the resulting collapsing protostar and protoplanetary disk. Given the problems with AGB and WR star winds [4], a SNR shock appears to be the leading contender for achieving simultaneous triggering and injection of supernova-derived short-lived radioisotopes (SLRIs, e.g., ⁶⁰Fe and ²⁶Al) into the presolar cloud and the resulting solar nebula [8].

Evidence for live ⁶⁰Fe during the formation of refractory inclusions and chondrites has waxed and waned in recent years. Data on ferromagnesian chondrules from two ordinary chondrites (OC) implied initial ⁶⁰Fe/⁵⁶Fe ratios of $\sim 5 - 10 \times 10^{-7}$ [9], whereas bulk sample data from a wide range of meteorites suggested an initial ratio of $\sim 1.15 \times 10^{-8}$ [10]. A combined study of ⁶⁰Fe and ²⁶Al in chondrules from unequilibrated OC (UOC) implied an initial ⁶⁰Fe/⁵⁶Fe ratio of $\sim 7 \times 10^{-7}$ [11] and supported a SNe as the source of the SLRIs. Analyses of other chondrules from UOC yielded ratios in the range of $\sim 2 - 8 \times 10^{-7}$ [12]. While there is as yet no explanation for the discrepancy between bulk samples and chondrule fragments [12], a SNe remains as a plausible source for the SLRIs. Indeed, evidence for possible live ¹³⁵Cs in CAIs suggests its origin in a Type II SNe (or its WR progenitor) close to the presolar cloud [13]. Furthermore, the evidence for live ¹⁰Be in FUN-CAIs appears consistent with ¹⁰Be formation in the presolar molecular cloud by galactic cosmic rays (GCRs) emitted by a SNR that thereafter triggered the collapse of the presolar cloud core [14]. Statistical analysis of the SLRI enrichments expected for disks and cloud cores in clusters containing massive stars showed that cloud cores receive a larger dose on average than disks

[15], favoring the presolar cloud scenario [8] over injection into a previously formed solar nebula [16].

Given this strong support for the triggering and injection hypothesis for the origin of the SLRIs, we continue to calculate increasingly detailed models of the hydrodynamics of the shock-cloud interactions, in order to further understand the physics of the process. Our previous work in both 2D [4] and 3D [6] considered rotating presolar clouds, capable of collapsing to form protostellar disks. Because of symmetry constraints in 2D, these models assumed that the cloud rotation axis was *parallel* to the direction of shock wave propagation. For ease of comparison, our first 3D rotating cloud models [6] made this same assumption. Here we present the results of a set of 3D models identical to previous rotating cloud models, but with the rotation axis *perpendicular* to the shock front direction. We start with $2.2 M_{\odot}$ cores with radii of 0.053 pc, rotating at either $\Omega = 10^{-14}$ or 10^{-13} rad s⁻¹. Shock speeds are $v_s = 20$ or 40 km s⁻¹, shock widths are 3×10^{-4} pc, and shock densities (ρ_s) are 7.2×10^{-18} g cm⁻³. The figures show the results for these four models, denoted by their v_s and Ω values. Central protostars and disks form in all models, though with disk spin axes deflected considerably. Injection efficiencies, f_i , defined as the fraction of the incident shock wave material injected into the collapsing cloud core, are ~ 0.03 in these models, as before [5,6]. Evidently altering the rotation axis orientation has only a minor effect on the outcome.

References: [1] Sashida, T., et al. (2013), ApJ, 774, 10. [2] Reach, W. T., et al. (2005), ApJ, 618, 297. [3] Blair, W. P., et al. (1999), AJ, 118, 942. [4] Boss, A. P., & Keiser, S. A. (2013), ApJ, 770, 51. [5] Boss, A. P., & Keiser, S. A. (2012), ApJL, 756, L9. [6] Boss, A. P., & Keiser, S. A. (2014), ApJ, 788, 20. [7] Li, S., et al. (2014), MNRAS, 444, 2884. [8] Boss, A. P. (1995), ApJ, 439, 224. [9] Tachibana, S., et al. (2006), ApJ, 639, L87. [10] Tang, H., & Dauphas, N. (2012), EPSL, 359-360, 248. [11] Mishra, R. K., & Goswami, J. N. (2014), GCA, 132, 440. [12] Mishra, R. K., & Chaussidon, M. (2014), EPSL, 398, 90. [13] Bermingham, K. R., et al. (2014), GCA, 133, 463. [14] Tatischeff, V., et al. (2014), ApJ, 796, 124. [15] Adams, F. C., et al. (2014), ApJ, 789, 86. [16] Ouellette, N., et al. (2007), ApJ, 662, 1268.

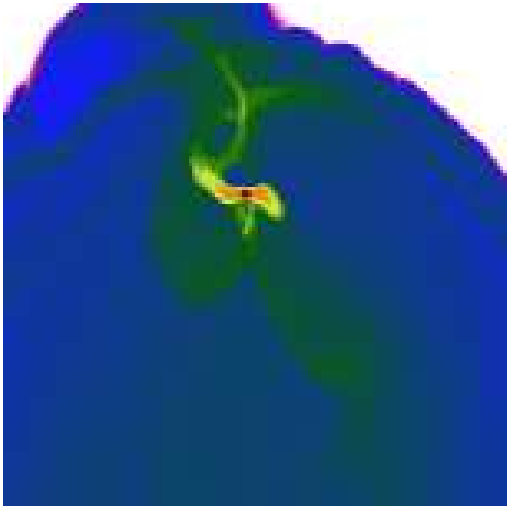


Fig. 1. Model 40-13 log density ($\rho_{max} \sim 10^{-11} \text{ g cm}^{-3}$) cross-section showing edge-on disk. Region shown is 1333 AU across at 0.086 Myr.

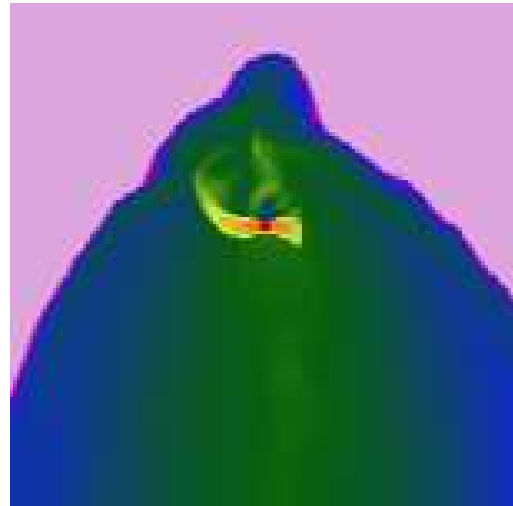


Fig. 2. Model 40-14 log density, plotted as in Fig. 1, at 0.079 Myr. Direction of initial spin axis is to the right in each model.

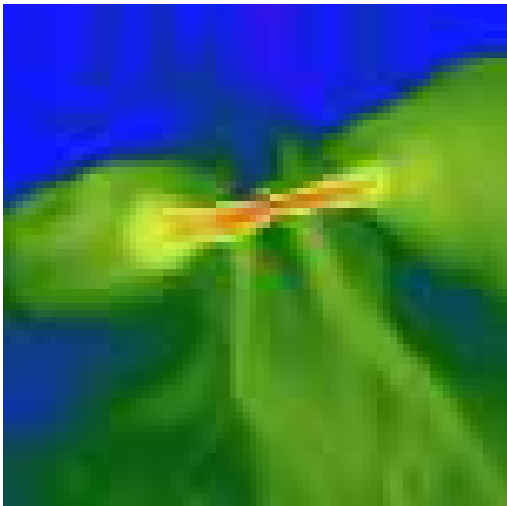


Fig. 3. Model 20-13 log density, plotted as in Fig. 1 at 0.15 Myr. Shock propagated from top to bottom in each model.

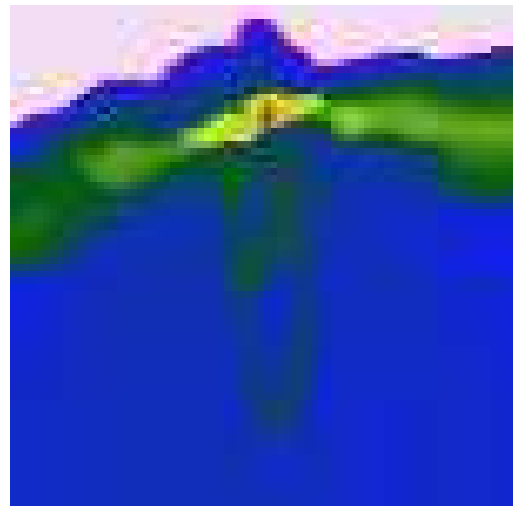


Fig. 4. Model 20-14 log density, plotted as in Fig. 1, at 0.13 Myr. Spin axes of the resulting disks are deflected from their initial directions.